Microstructural variation through weld thickness and mechanical properties of peened friction stir welded 6061 aluminum alloy joints

Mustafa A. Abdulstaar, Khaled J. Al-Fadhalah, Lothar Wagner

PII: S1044-5803(16)30588-5
DOI: doi: 10.1016/j.matchar.2017.02.011
Reference: MTL 8563

To appear in: *Materials Characterization*

Received date: 17 October 2016
Revised date: 21 January 2017
Accepted date: 11 February 2017

Please cite this article as: Mustafa A. Abdulstaar, Khaled J. Al-Fadhalah, Lothar Wagner , Microstructural variation through weld thickness and mechanical properties of peened friction stir welded 6061 aluminum alloy joints. The address for the corresponding author was captured as affiliation for all authors. Please check if appropriate. Mtl(2017), doi: 10.1016/j.matchar.2017.02.011

Microstructural Variation through Weld Thickness and Mechanical Properties of Peened Friction Stir Welded 6061 Aluminum Alloy Joints

Mustafa A. Abdulstaar[a,*] mustafa.abdulstaar@tu-clausthal.de, Khaled J. Al-Fadhalah[b], Lothar Wagner[a] mustafa.abdulstaar@gmail.com

[a]Institute of Material Science and Engineering, Clausthal University of Technology, Agricolastr. 6, 38678 Clausthal-Zellerfeld, Germany

[b]Department of Mechanical Engineering, College of Engineering & Petroleum, Kuwait University, P.O. Box 5969, Safat, 13060, Kuwait

[*]Corresponding author.

Abstract

The current study examined the effect of microstructure variation on the development of mechanical properties in friction stir welded joints of 6061-T6 aluminum alloy, which were subsequently processed by shot peening (SP). Following to FSW, fatigue specimens were extracted perpendicularly to the welding direction. Surface Skimming to 0.5 mm from crown and root sides of the joint was made and SP was later applied on the two sides using ceramic shots of two different Almen intensities of 0.18 mmA and 0.24 mmA. Microstructural examination by electron back scattered diffraction (EBSD) indicated variation in the grain refinement of the weld zone, with coarsest grains (5 μm) at the crown side and finest grains (2 μm) at the root side. Reduction of microhardness to 60 Hv occurred in the weld zone for samples in FSW condition. Application of SP promoted significant strain hardening at the crown side, with Almen intensities of 0.24 mmA providing maximum increase in microhardness to 120 Hv. On the contrary, only a maximum microhardness of 75 HV was obtained at the root side. The difference in strain hardening capability at the two sides was strongly dependent on grain size. The two Almen intensities produced similar distribution of compressive residual stresses in the subsurface regions that led to enhance the fatigue strength to the level of base metal for $N \geq 10^5$ cycles. Yet, the increase in fatigue strength was more pronounced with increasing Almen intensity to 0.24 mmA, demonstrating further enhancement by strain hardening.

Keywords: Aluminum alloys, friction stir welding, shot peening, fatigue, microstructure

Abstract

The current study examined the effect of microstructure variation on the development of mechanical properties in friction stir welded joints of 6061-T6 aluminum alloy, which were subsequently processed by shot peening (SP). Following to FSW, fatigue specimens were extracted perpendicularly to the welding direction. Surface Skimming to 0.5 mm from crown and root sides of the joint was made and SP was later applied on the two sides using ceramic shots of two different Almen intensities of 0.18 mmA and 0.24 mmA. Microstructural examination by electron back scattered diffraction (EBSD) indicated variation in the grain refinement of the weld zone, with coarsest grains (5 μm) at the crown side and finest grains (2 μm) at the root side. Reduction of microhardness to 60 HV occurred in the weld zone for samples in FSW condition. The two Almen intensities produced similar distribution of compressive residual stresses in the subsurface regions. SP with an Almen intensity of 0.24 mmA promoted significant strain hardening at the crown side, resulting in a maximum microhardness of 120 HV. On the contrary, only a maximum microhardness of 75 HV was obtained at the root side. The difference in strain hardening at the two sides was strongly dependent on grain size. SP also led to formation of tensile residual stresses in the mid-thickness of the weld joint that resulted in unexpected softening. The large compressive residual stresses in the subsurface regions enhanced the fatigue strength to the level of base metal for $N \geq 10^5$ cycles. Yet, the increase in fatigue strength was more pronounced with increasing the Almen intensity to 0.24 mmA, demonstrating further enhancement by strain hardening.

Keywords: Aluminum alloys, friction stir welding, shot peening, fatigue, microstructure

1. Introduction

Since its invention as a solid-state joining process in the early 1990s [1], friction stir welding (FSW) has been widely used to join several aluminum alloys and other metallic alloys that are difficult to bond by conventional fusion welding. Due to the low heat input and stress accommodation by recrystallization that occur during FSW, it is anticipated that low residual tensile stresses are generated in the weld joint. Early studies showed that maximum residual stresses in FSW welds of various aluminum alloys were below 100 MPa, which are much lower than those observed in fusion welding [2-5]. Despite that, the use of rigid clamping in FSW causes an additional restraint on the welded plates, which impedes the contraction of the weld nugget and heat-affected zone (HAZ) during cooling and thus signifies the effect of residual stresses [6]. Also, the magnitude and distribution of residual stresses developed by FSW can significantly influence the structural integrity of weldments [7-8]. In particular, the tensile residual stresses in the weld nugget and surroundings can have detrimental effects on the fatigue performance by facilitating fatigue micro-cracks propagation [9] and developing sites for fatigue crack nucleation [10]. Extensive reviews have been made to examine the effect of FSW on microstructure, residual stress and mechanical properties for different metallic alloys [6,11], suggesting that FSW weld joints have superior fatigue strength to that of conventional fusion welded joints but inferior to that of base material (BM) in most cases. It was also reported that the reduction in the fatigue strength is primarily due to material softening and/or tensile residual stresses arising from FSW.

Shot peening (SP) has been widely used as an effective method to enhance the fatigue performance of welded joints. The process of SP generally requires bombardment of the metal substrate by high velocity shots made from metals or ceramics, which induces compressive residual stresses in the surface and near-surface layers and hence enhances the fatigue performance [12,13]. A major drawback of the SP process is the high surface roughness in comparison to other surface treatments like ball-burnishing or ultrasonic shot peening [14,15], where fatigue micro-crack could be initiated from the narrow depression of peening dimples.

Nevertheless, compressive residual stresses play an important role in hindering or even suppressing the fatigue micro-crack propagation from the surface towards the interior [16]. In recent years, there has been a great interest in optimizing the fatigue performance of FSW aluminum alloys, for the use in fatigue load bearing structures, by shot peening and other advanced peening methods. Ali et al. [17] examined the effect of SP on fatigue behavior of FSW AA 2024, the study shows that significant improvement in fatigue life both in the region of low and high cycle fatigue. It was reported that SP concentrated the crack initiation sites into the nugget zone more than ~~in~~ the thermomechanical affected zone (TMAZ) or HAZ, and also resulted in slow near surface crack propagation due to the compressive residual stresses induced by SP. Moreover, Hatamleh and coworkers [18,19] made comprehensive examination of the effect of different surface treatments (as weld, shot peening, and laser peening LP) on fatigue performance of FSW AA 2195 joints. It was concluded that joints in peened condition had improved distribution of compressive stresses that found to be responsible for increasing the resistance to fatigue crack growth. However, LP had markedly deeper compressive residual stresses through sample thickness as compared to SP conditions. Another study by Hatamleh et al. [20] on FSW joints of AA 2195 and AA 7075 also showed that SP lead to higher magnitude of compressive residual stresses on the outer surface compared to LP due to high amount of cold work in SP process, unlike the sub-surface region where higher and deeper compressive residual stresses were obtained from LP. In addition, Sano et al. [21] studied the effect of LP on FSW joints of AA 6061-T6 and indicated that bending fatigue strength at (stress ratio R = -1) is highly improved in LP condition as compared to the as-weld joint, exceeding the fatigue strength of the base metal. However, this improvement in fatigue strength occurred in the high-cycle fatigue (HCF) regime and become less significant in the low-cycle fatigue regime. A recent study on shot peening of FSW joints of AA 6061-T6 [22] reported fatigue enhancement in HCF regime for samples in SP condition to the same as that of base metal. The fatigue life was also dramatically improved by SP for all stress levels as

compared to that in FSW condition.

The above studies distinctly indicated the enhancement of fatigue properties by shot peening of several aluminum alloys weld joints made by FSW. Despite that, the new findings presented in the current study are linking the formation of inhomogeneous microstructures in the FSW joint to the evolution of mechanical properties, particularly after SP. FSW was applied to make AA 6061-T6 welded joints that were subsequently processed by surface skimming and SP. Surface skimming was made to the crown and root sides of the joint to avoid stress concentration and surface irregularities created by the welding tool. To optimize fatigue performance of the welded joint, SP was applied to the crown and root sides using two Almen intensities. For both FSW and SP conditions, the variation of microstructure through the thickness of weld joint was examined using optical microscopy (OM) and electron back scattered diffraction (EBSD). The effect of SP on the evolution of residual stresses in the weld joint was studied. The microhardness and fatigue properties of the welded joint were also evaluated.

2. Experimental Procedure

Aluminum alloy 6061-T6 plates were used in this study to conduct FSW experiments. The FSW plates have a thickness of 4 mm with an area of 60 mm by 300 mm as schematically illustrated in Fig. 1a. The FSW tool is made of D2 tool steel, which has a shoulder of 15 mm diameter and a straight cylindrical pin being 4 mm in length and 4 mm in diameter. The FSW was made in a direction perpendicular to the rolling direction of the AA 6061 plates, which were clamped in a butt-weld configuration on a backing anvil of low carbon steel. The FSW was conducted using a vertical milling machine and the tool was plunged into the abutting edges of the two plates and traversed along the edges with a constant tool rotating rate of 1200 rpm, a travel speed of 50 mm/min and a pitch angle of 2 degrees. To examine the effect of surface skimming on fatigue performance, both crown and root sides of the welded plates were machined by 0.5 mm using milling machine. The skimming was done using milling

machine to remove any surface irregularities resulting from the welding process that could affect the fatigue results.

The SP process was conducted using a gravity-induction shot peening machine (model: OSK-Kiefer GmbH). This type of SP machine allows the shots to be elevated above the point of usage, permitting them to free fall towards the nozzle where they are energized using compressed air. Spherical ceramic shots (Z300) composed of 67% ZrO_2, 30% SiO_2 and 3% others, were used in this study with an average shot size of 0.36 mm and hardness of 780 HV_1. Peening was performed on crown and root sides of the weld zone to full (100%) coverage, and two Almen intensities were used (0.18 mmA and 0.24 mmA). The Almen intensity was determined from the arc height of Almen strip using an Almen gauge.

Microstructural refinement in the stir zone was assessed through thickness for samples in FSW and SP conditions. Metallographic samples were prepared for examination by using optical microscopy (OM) and Electron Backscattered Diffraction (EBSD) technique. The samples were cut from the cross-section of the plates normal to the welding direction, i.e. ND-TD plane, then ground and polished using standard metallography techniques. Examination by OM was carried out using a stereomicroscope (model: Ziess, Stemi 2000) and the samples were chemically etched at ambient temperature for about six minutes with an extended Flick reagent consisting of 1.5 parts of HCl, one part of HF and nine parts of H_2O [23]. The EBSD analysis was conducted using HKL5 EBSD system interfaced with a JEOL 7001F-JSM FE-SEM and operated at 20 kV. EBSD samples were prepared using Struers (LectroPol-5) electro-polishing unit with an electrolyte A2 at 25°C with an applied potential of 24 V. EBSD maps were made at 1000X magnification and using a step size of 0.3-0.4 μm. As schematically illustrated in Fig.1b, the development of microstructure by FSW was first evaluated across the weld zone in the advancing side, starting from the stir zone (SZ) and passing through the TMAZ towards the BM. In addition, EBSD measurements were made at different depths of the stir zone to evaluate microstructure variation in SZ. In particular,

measurements were made to examine the evolution of microstructure by FSW and SP along the centerline of the weld as follows (see Fig.1b): 1 mm below the crown surface (line A-A), middle of the sample thickness (line B-B), and 1 mm above the root surface (line C-C). The misorientation angle distribution statistics was analyzed, employing a critical misorientation angle of 15° to differentiate low-angle boundaries (LABs) from high-angle boundaries (HABs). The grain boundaries are presented in EBSD maps such that LABs are depicted as thin grey lines and HABs as solid black lines. The average grain size was calculated according to ASTM: E112, using an average intercept method program available with the EBSD software. Also, kernel average misorientation (KAM) analyis was made to evaluate the variation of local strain in different regions of SZ due to shot peening. KAM maps were constructed by computing the average misorientation between each measurement point and its neighbors, excluding grain boundaries with misorientation angle higher than 5°.

To correlate the evolution of microstructure with mechanical properties, the hardness of FSW and SP samples were evaluated across the weld zone by Vickers microhardness testing. The indentations were made using a Vickers microhardness tester (model: Buehler, Micromet) on metallographically prepared specimens under a load of 100 gf and for dwell time of 20 seconds. As illustrated in Fig.1b, three indentations lines (line A-A, line B-B and line C-C) were made horizontally across the weld zone using an increment of 0.5 mm. In addition, tensile testing was performed using dog-bone shaped specimens; the tensile properties of base metal and FSW condition are summarized in Table 1. Moreover, fatigue testing was performed to evaluate the effect of shot peening using an alternating bending fatigue device (model: Carl Schenck AG). The size and shape of the flat bending fatigue specimen is schematically illustrated in Fig. 2. The fatigue specimens were extracted from the base material and the friction stir welded material (Fig. 1) using electric discharge machining EDM, wet grinded using SiC paper was applied to eliminate the traces created by EDM process. The thickness of each fatigue specimen was 3 mm after removing 0.5 mm from the

crown and root sides. The fatigue loading was applied in direction perpendicular to the welding direction with stress ratio of R = -1 and with a testing frequency of 24 Hz (1420 rpm). The surface roughness of samples in FSW and SP conditions was determined by means of an electronic contact stylus profilometer instrument (model: Perpethometer S8P). For each condition, the average of three roughness measurements was taken.

Residual stresses were determined by means of the incremental hole drilling method using a drill with a diameter of 1.9 mm and strain gage rosettes according to ASTM E837-13a (model: MTU Aero Engines GmbH). The oscillating drill was driven by an air turbine at a rotational speed of 2×10^5 rpm. The residual stress measurements were made at the center of the weld joint and starting from the top surface to a depth of 1.1 mm.

3. Results and discussion

3.1 Surface Roughness

Surface skimming was applied by machining 0.5 mm from the crown and root sides of the FSW joint to remove surface irregularities and tool marks. SP was later applied directly to the machined surface. Fig. 3 presents the maximum roughness height (R_z) for samples in FSW and SP conditions. Machining resulted in relatively smooth surfaces for FSW sample (R_z = 1.6 µm). Additional treatment by SP with Almen intensity of 0.18 mmA on the machined surfaces resulted in high roughness value (R_z = 5.9 µm). The use of Almen intensity of 0.24 mmA was also found to make the surface rougher (R_z = 7.7 µm). The increase in surface roughness might result in stress concentration during fatigue testing, which will be further examined in the discussion of fatigue performance.

3.2 Residual stresses

Fig. 4 illustrates the distribution of residual stress in longitudinal and transverse direction through the joint thickness for various investigated conditions. The measurements of residual stresses were made on the crown side at the weld center. The results show a minor

difference in residual stresses values between the longitudinal and transverse direction. The residual stress state in the BM is ranging from -20 MPa to -10 MPa without huge values scattering up to 0.6 mm depth. For sample in FSW condition, the residual stress tends to be tensile beneath the outer surface and reached its maximum value of about 200 MPa at depth of 0.2 mm, and later the tensile residual stress declined as the depth increases. The measured value for the maximum tensile stress is relatively high. This might due to the sensitivity of incremental hole drilling technique for measuring tensile residual stresses, as compared to other more accurate measuring technique like X-ray diffraction. For sample SP by intensity of 0.18 mmA, a remarkable compressive residual stresses formed at the crown surface (at 0.04 mm depth), reaching a maximum value of -210 MPa. The compressive residual stress becomes less and reaches zero at a depth of 0.6 mm. The maximum tensile residual stress occurs at depth of 0.89 mm, reaching about 104 MPa that is being two times lower than that obtained in FSW condition. It was reported [24] that mechanical surface treatments like SP or ball-burnishing induce tensile residual stresses to balance the compressive residual stresses at the outer surface. The residual stress turns again into compressive stress approximately at depth of 1.05 mm. SP with higher intensity (0.24 mmA) resulted in maximum compressive residual stress of about -241 MPa at 0.06 mm depth. The zero crossing depth was recorded at 0.56 mm depth, while maximum residual tensile stress was found to be 117 MPa at 0.66 mm depth. Compared to SP by 0.18 mmA, higher tensile residual stress and less zero crossing depth were obtained by using 0.24 mmA intensity. This is could be related to balancing the higher compressive stresses at the near-surface region. In general, SP revealed a significant role in terms of hindering the effect of tensile residual stress state observed in FSW condition. The application of SP on both crown and root side of FSWed joint was shown to introduce compressive residual stresses and thereby enhance material resistance against fatigue propagation from the surfaces of the weld joint.

3.3 Microstructure

Fig. 5 represents a low-magnification overview of the transverse cross section of the FSW joint. Four distinct zones can be identified: SZ, TMAZ, HAZ and BM. The SZ has a basin-like shape significantly widening towards the upper surface due to the forging effect of the tool shoulder on material flow during FSW. No clear distinction was observed between TMAZ and HAZ and also there is no clear kissing bond is formed in root side and even if it is formed it gets removed by surface skimming process. Fig.6 also shows OM micrographs at the SZ-TMAZ interface for FSW sample, demonstrating that TMAZ represent a narrow zone extending to about 200 µm from the interface. Moreover, the microstructure at the interface between SZ and TMAZ for sample in FSW condition is further examined by EBSD as shown in Fig.7. The EBSD mapping was made approximately at middle plane (center line). The results show a remarkable grain refinement in the SZ with an average grain size of 2.9 µm. The SZ is characterized by large formation of high angle grain boundaries (HABs), with a frequency of 69%. The TMAZ is characterized by deformed microstructure, as demonstrated by low-angle grain boundaries (LABs) shown in grey, with a larger grains having an average size of 7.1 µm. The grains in HAZ are coarser with an average size of 10.9 µm, but they are characterized by lesser amount of LABs than that in TMAZ due to the effect of heating by FSW.

The effect of shot peening on the microstructure development of the SZ has also been examined in Fig.8. For each processing condition, EBSD maps were made at the center line of the weld at three positions (top, middle, and bottom of the weld joint). Measurements at the top and bottom positions were made 100 µm beneath the surface. In general, the results demonstrate variation of the grain size in the SZ of FSW sample through the weld thickness, being largest at the top and smallest at bottom. Having coarser grains at the top is most likely to occur due to the additional heating by friction between the shoulder and sample surface, giving a rise for extra heating time during thermal cycle of FSW. Similar trend in grain

refinement can also be observed for shot peened samples, which demonstrates that SP has generally introduced limited change in the overall microstructure. However, a close look into the statistics of the average grain size and fraction of HABs, shown in Table 2, provides additional information on the microstructural development at different depths of the SZ. At the top of the weld joint, the size of grains has barely changed by the shot peening treatment having an average size of approximately 5 μm, while there is a moderate increase in the HABs fraction (from 60% for FSW sample to 66% for sample SP by 0.24 mmA). This might be associated with the evolution of the LABs, originally formed in the FSW microstructure, into HABs due to strain hardening of the shot-peened top surface. Lee et al. [25] reported that SP of steel weld induces strain hardening below the surface. This was demonstrated by the formation of sub-boundaries via evolution of dense dislocation wall and dislocation tangles, and later resulting in formation of HABs. On the other hand, the average grain size at the middle and bottom sections slightly increased with the application of SP. The average grain size at the middle (bottom) section increases from about 3.2 (1.6) μm at FSW condition to 3.9 (2.1) after SP by 0.24 mmA intensity. The slight increase in grain size by SP at middle and bottom sections is strongly associated to the reduction in the fraction of HABs as presented in Table 2. The fraction of HABs was initially high in the FSW microstructure at the middle and bottom sections (69% and 85%, respectively) and additional deformation by SP resulted in a reduction in the HABs fraction (62% and 81%, respectively). Furthermore, the current shot peening treatment was not shown to cause a significant rise in temperature and thus it is not expected to induce significant microstructural changes such as grain growth. Therefore, it is suggested that SP caused little variation in the grain size and HAGs fraction of the FSW joint. Such variation is thought to be related to the differences in strain hardening shown at different regions of the joint.

Fig. 9 shows kernel average misorientation (KAM) maps highlighting local strain variations in the SZ for samples in FSW and SP conditions. Brighter pixels indicate positions of abrupt orientation change in the microstructure. These typically present groups of grain boundaries of low misorientation angles and they are most likely interpreted as dislocation arrays. In general, there is an increase in local strain variations with increasing shot peening intensity. The variations in local strain occurred more pronouncedly at the top and bottom regions due to the direct impact of shot peened particles at these surfaces that induced plastic deformation and thus possible storage of dislocations as LABs. In the mid-thickness region, lower variations in local strain are shown to occur than that observed in top and bottom regions. In such a case, plastic deformation by shot peening is not expected to occur in this region since the peening effect does not generally exceed the diameter of the peening indentations. Instead of that, a variation in local strain is expected to occur due to the presence of tensile residual stresses, which was found to form in the mid-thickness region to balance the compressive residual stresses formed in the top and bottoms regions.

3.3 Microhardness

Fig. 10 shows the distribution of microhardness across the weld zone and through depth in three different regions (center, top and bottom). The results for FSW sample shown in Fig.10a indicate a softening in the weld joint, from the SZ towards HAZ, in comparison to the unaffected BM that has an average microhardness of 115 HV. The softening extends to about 10 mm from the center of the weld with a minimum of 60 HV. Also, the severest softening occurs for the measurements made at the top of the weld joint. This is most likely due to the direct contact with the shoulder of the tool that generated additional frictional heat and extended the size of the SZ, as compared to the bottom of the weld. A previous study on FSW of Al6063 reported that the softening in SZ and HAZ is due to the dissolution or partial dissolution of needle-shaped β'' precipitates [26]. It was found that the severity of softening

mainly depends on the temperature field generated by the welding process. The softening in the processed zone for 6000 series aluminum alloys was also documented in other FSP/FSW studies [27,28]. Moreover, the microhardness profiles for samples in SP condition are shown in Fig.10b and 10c. The results show that SP generally caused hardness enhancement in SZ more effectively than in TMAZ and HAZ. The hardness enhancement was most affective on the top surface, moderate on the bottom surface and least effective at the center of weld joint. The maximum hardness occurred at the top region, reaching a value of 105 Hv for sample peened with an intensity of 0.18 mmA (Fig. 10b) and about 120 HV for sample peened with an intensity of 0.24 mmA (Fig. 10c). On the other hand, maximum hardness at the bottom region did not exceed 75 HV for both Almen intensities. Such differences in strain hardening by SP are thought to be related to the variation in grain size in different regions of the SZ. For FSW condition, the average grain size in top region is about 5 μm, while it is reduced to 1.8 μm in the bottom region. Sun et al. [29] examined the effect of initial grain size, from 0.47 to 20 μm, on strain hardening of commercial pure aluminum. It was found that higher strain hardening rate occurred for samples with coarser grains as compared to their counterparts of smaller grains. In the case of large grains, it was suggested that there is enough space for significant dislocation intersections during deformation. For smaller grains, dislocations had less chance to interact as they deposited on opposite boundaries directly, thus resulting in minimal hardening. Moreover, the increase in the SZ hardness was influenced by the dynamic strain hardening occurring by the repeated impacts of the ceramic shots during SP surface treatment, unlike the deformed and/or thermally-affected microstructure in TMAZ and HZ that were less capable to harden [21]. Previous studies on shot peening of AA 2024 [13] and AA 6082 [30] indicated that less strength improvement after SP occurred for sample in T6 condition as compared to SP of the same material but in T4 condition. This explains the relatively low strain hardening by SP in TMAZ and HAZ for the current aluminum alloy in which the base metal is in T6 temper condition.

The evolution of SZ hardness at different weld depths is further illustrated in Fig. 11. The results show that shot peening remarkably enhanced the hardness of SZ at the top region, while limited improvement occurred at the bottom region. This is consistent with a previous study by Sano et al. on laser peening of FSW joint of AA 6061 [21]. The difference in hardness enhancement by SP is also influenced by the width of SZ at the two regions, being wide at the crown side and narrow at the root side. Fig. 11a & 11c also demonstrates that work softening in BM occurred at the top and bottom surfaces at a distance greater than 10 mm from the weld center. This type of softening by shot peening was reported in previous studies [31-33], indicating that work softening by SP favorably occurred for pre-strained metals. In such case, the accumulation of large strain by multiple impact of shots on the peened surface reaches a level at which the rate of dislocation generation equals the rate of annihilation. In spite of having compressive residual stresses in the peened region, further straining by SP induces work softening and thus a reduction in the hardness. Moreover, Fig. 11b presents the hardness evolution at the mid-thickness region and indicates that SP generally resulted in a reduction in the hardness as compared with sample in FSW condition. An increase in the hardness is only confined to small distance from the weld centerline. The results also show that softening at the mid-thickness region becomes more pronounced with increasing Almen intensity, spreading horizontally over wider distance from the center line (Fig. 10b & 10c). This type of softening is most likely attributed to the presence of tensile residual stresses. This is possible since plastic deformation is usually confined to the peened-surface regions, and thus it is not expected to have strain hardening in the mid-thickness region. Tosha [34] examined the effect of residual stresses produced by bending and tensile tests on hardness distribution in carbon steel, indicating an increase in the hardness in regions of compressive residual stresses and hardness reduction in regions of tensile residual stresses. SP was also made on carbon steel resulting in an increase in the hardness in the peened regions due to the formation of compressive residual stresses.

The current results suggest that the inhomogeneity of microstructure by FSW and the change in residual stress distribution by SP remarkably influences the evolution of hardness in the weld joint. SP was shown to cause large compressive residual stresses at the top and bottom sides resulting in strain hardening in the SZ-HAZ and surprisingly softening of the BM. For the mid-thickness region, the tensile residual stresses due to SP led to softening in the SZ-HAZ. Softening in the mid-thickness was also found to occur in the BM, at a distance greater than 10 mm from the center line. This type of softening is similar to that detected at the top and bottom sides in the BM region far away from the SZ. This suggests that the use of SP at the crown and root sides of the weld joint induced large amount of strain.

3.5 Fatigue performance

Fig. 12 presents the fully reversed (R = -1) plane bending fatigue behavior of AA 6061 in FSW and SP conditions, plotted as stress amplitude (S) versus number of fatigue cycle (N_f). The fatigue strength of the BM is 100 MPa at 10^7 cycles. The results also show that failure at given N_f occurs at lower stress amplitude for sample in FSW condition, as compared to that for BM sample. This is mainly attributed to the softening in the joint, particularly in SZ, which took place during welding process (Fig. 10a) and also the presence of large residual tensile stresses at the near-surface regions (Fig. 11). On the other hand, SP by an intensity of 0.18 mmA resulted in restoration of fatigue resistance to the BM at HCF regime. This is demonstrated as both samples, BM and SP by 0.18 mmA, have similar fatigue strength of 100 MPa at 10^7 cycles. The increase in the Almen intensity to 0.24 mmA caused further enhancement in fatigue strength to 125 MPa. It can also be noticed that SP has more pronounced fatigue improvement at low stress amplitude compared to high stress amplitude regime. This is due to the cyclic stability of compressive residual stresses at low stress amplitude values found in HCF regime, as compared to the relaxation in compressive residual stresses at high stress amplitude in LCF regime. Besides the introduction of compressive residual stresses, the enhancement of fatigue performance by SP is strongly related to strain

hardening and that were induced at the surface and near-surface regions. Strain hardening offers a significant barrier against fatigue crack nucleation, while compressive residual stresses retard the fatigue crack propagation [16].

Sano et al. [21] studied the effect of laser peening on fatigue performance of AA 6061-T6 FSWed joints. LP was applied directly to the FSWed fatigue specimens without prior surface skimming. The results showed an improvement in fatigue performance of FSW condition after applying LP only at $N \geq 10^6$ cycles, for which the fatigue strength exceeded that of BM. For $N \leq 10^5$ cycles, the fatigue strength was much less than BM. Another study by Masaki et al. [22] also indicated an increase in fatigue strength of shot-peened FSWed joints of AA 6061-T6 to the same value of base material but only at HCF regime ($N \geq 10^6$ cycle). Moreover, the effect of skimming on fatigue performance was reported on a previous study on FSW of AA 2024-T3 [17]. Applying shot peening after surface skimming was shown to result in remarkable enhancement of fatigue life as compared to shot peening of un-skimmed specimens. Also, peening after skimming was found to provide a better overall fatigue life than the BM, particularly in the HCF region. In the present study, it has been demonstrated that the use of surface skimming and SP together play an important role in the enhancement of fatigue performance of FSW joints to the level of BM for both low and high cycle regimes. In addition, the fatigue performance was further improved with increasing the intensity from 0.18 mmA to 0.24 mmA.

4. Conclusions

Combined surface skimming and shot peening was performed on friction stir welded joints of aluminum 6061-T6 alloy. The microstructure, residual stresses, microhardness and fatigue performance were evaluated and the followings conclusion remarks were derived:

1. Residual stress-depth profile for FSW sample, measured at the weld centerline, indicates tensile residual stresses peak at 0.2 mm depth from the crown surface. SP was shown to result in large subsurface compressive stress of -220 MPa and -241

for 0.18 mmA and 0.24 mmA intensity, respectively. This was balanced by tensile residual stress at depth ranging from 0.5 to 1.0 mm.

2. FSW introduced varying microstructural refinement in the SZ of the weld joint. Higher fraction of HAGs formed in the bottom region of the SZ that resulted in fine grains with an average size of 1.6 μm. In the top region of the SZ, the additional heat provided by FSW tool shoulder provided coarser grains with an average size of 5 μm; this was also found to correlate with the lower fraction of HAGs. SP was found to cause limited changes in the SZ microstructure.
3. A remarkable reduction in the SZ hardness occurred, particularly at the crown side of the FSW joint, reaching 60 HV that is approximately half the hardness of the BM. This is attributed to dissolution of strengthening precipitates and the additional heating by the friction between the tool shoulder and the crown surface of the joint. Increasing Almen intensity of SP resulted in an increase in the SZ hardness at the two sides of the joint due to strain hardening and formation of compressive residual stresses. On the other hand, the generation of tensile residual stresses at the mid-thickness of the SZ led to softening. Also, the use of SP at both surfaces induced large amount of strain in the BM region that resulted in work softening regardless to the presence of compressive residual stresses.
4. The fatigue strength of FSW samples remarkably decreases compared to that of base metal. The combined use of surface skimming and SP was effective in restoring the fatigue strength to the BM level. Increasing the Almen intensity from 0.18 mmA to 0.24 mmA further improves the fatigue strength.

Acknowledgments

The authors would like to acknowledge the support provided by Kuwait University General Facility project (GE 01/07) for sample preparation, optical microscopy, and EBSD measurements. Institute of materials science and engineering at Clausthal University of

Technology and German academic exchange service (DAAD) are gratefully acknowledged.

References

1. W.M. Thomas, E.D. Nicholas, J.C. Needham, M.G. Murch, P. Templesmith, C.J. Dawes, Friction stir butt welding, International Patent Application No. PCT/GB92/02203 and GB Patent Application No. 9125978.8, 1991.
2. M. James, M. Mahoney, D. Waldron, Residual Stress measurements in friction stir welded aluminum alloys, Proc. 1st Int. Symp. on Friction Stir Welding, Thousand Oaks, CA, USA, 1999.
3. C.D. Donne, E. Lima, J. Wegener, A. Pyzalla, T. Buslaps, Investigation on residual stresses in friction stir welds, Proc. 3rd Int. Symp. on Friction Stir Welding, Kobe, Japan, 2001.
4. X. Wang, Z. Feng, S. David, S. Spooner, C. Hubbard, Neutron diffraction study of residual stresses in friction stir welds, Proc. 6th Int. Conf. on Residual Stresses (ICRS-6), p. 1408, IOM Communications, Oxford, UK, 2000, pp. 1408-1420.
5. M. Peel, A. Steuwer, M. Preuss, P.J. Withers, Microstructure, mechanical properties and residual stresses as a function of welding speed in aluminum, Acta. Mater. 51 (2003) 4791-4801.
6. R.S. Mishra, Z.Y. Ma, Friction stir welding and processing, Mater. Sci. Eng. R 50 (2005) 1-78.
7. G. Bussu, P.E. Irving, The role of residual stress and heat affected zone properties on fatigue crack propagation in friction stir welded 2024-T351 aluminum joints, Int. J. Fatigue. 25 (2003) 77-88.
8. M.B. Prime, T. Gnaupel-Herold, J.A. Baumann, R.J. Lederich, D.M. Bowden, R.J. Sebring, Residual stress measurments in a thick, dissimilar aluminum alloy friction stir weld, Acta. Mater. 54 (2006) 4013-4021.

9. L. Wagner, G. Luetering, V. Sadlacek, Fatigue crack growth retardation in an Al alloy 2024 in a residual compressive stresses, Proc. 2nd Int. Conf. on Residual Stresses, p. 803, Nancy, France, 1988 pp. 803-808.
10. A. Zammit, M. Mhaede, M. Grech, S. Abela, L. Wagner, Influence of shot peening on the fatigue life of Cu-Ni austempered ductile iron, Mater. Sci. Eng. A 545 (2012) 78-85.
11. A.L. Biro, B.F. Chenelle, D.A. Lados, Processing, microstructure and residual stress effects on strength and fatigue crack growth properties in friction stir welding: A review, Metall. Mater. Trans. B 43 (2012) 1622-1637.
12. A. Drechsler, T. Doerr, L. Wagner, Mechanical surface treatments on Ti-10V-2Fe-3Al for improved fatigue resistance, Mater. Sci. Eng. A 243 (1998) 217-220.
13. T. Ludian, L. Wagner, Effect of age-hardening conditions on high-cycle fatigue performance of mechanically surface treated Al 2024, Mater. Sci. Eng. A 468-470 (2007) 210-2013.
14. L. Wagner, M. Mhaede, M. Wollmann, I. Altenberger Y. Sano, Surface layer properties and fatigue behavior in Al 7075-T73 and Ti-6Al-4V: Comparing results after laser peening; shot peening and ball-burnishing, Int. J. Struct. Integr. 2 (2011) 958-968.
15. E. Maawad, H-G. Brokmeier, L. Wagner, Y. Sano, Ch. Genzel, Investigation on the surface and near-surface characteristics of Ti-2.5Cu after various mechanical surface treatments, Surf. Coat. Technol. 205 (2011) 3644-3650.
16. L. Wagner, Mechanical surface treatments on titanium, aluminum and magnesium alloys, Mater. Sci. Eng. A 263 (1999) 210-216.
17. A. Ali, X. An, C.A. Rodopoulos, MW. Brown, P. O'Hara, A. Levers, S. Gardiner, The effect of controlled shot peening on the fatigue behavior of 2024-T3 aluminum friction stir welds, Int. J. Fatigue 29 (2007) 1531-1545.

18. O. Hatamleh, A comprehensive investigation on the effects of laser and shot peening on fatigue crack growth in friction stir welded AA 2195 joints, Int. J. Fatigue 31 (2009) 974-988.
19. O. Hatamleh, M. Hill, S. Forth, D. Garci, Mater, Fatigue crack growth performance of peened friction stir welded 2195 aluminum alloy joints at elevated and cryogenic temperatures, Sci. Eng. A 519 (2009) 61-69.
20. O. Hatamleh, A. DeWald, An investigation of the peening effects on the residual stresses in friction stir welded 2195 and 7075 aluminum alloy joints, J. Mater. Process. Technol. 209 (2009) 4822-4829.
21. Y. Sano, K. Masaki , T. Gushi, T. Sano, Improvement in fatigue performance of friction stir welded A6061-T6 aluminum alloy by laser peening without coating, Mater. Des. 36 (2012) 809-814.
22. K. Masaki, K. Yamashiro, Y. Kobayashi, T. Tuji, Effect of shot peening with fine zirconia shot on fatigue property of friction stir welded A6061 alloy, J. Soc. Mater. Sci. 63 (2014) 596-601.
23. M. Schikorra, L. Donati, L. Tomesani, A.E. Tekkaya, Microstructure analysis of aluminum extrusion: Grain size distribution in AA 6060, AA 6082 and AA 7075 alloys, J. Mech. Sci. Technol. 21 (2007) 1445-1451.
24. E. Maawad, H.-G. Brokmeier, M. Hofmann, Ch. Genzel, L. Wagner, Stress distribution in mechanically surface treated Ti-2.5Cu determined by combing energy-dispersive synchrotron and neutron diffraction, Mater. Sci. Eng. A 527 (2010) 5745-5749.
25. W.B. Lee, G.H. Kim, K.I. Moon, Y. Lee, Strengthening dual phase steel welds by shot peening, ISIJ International 49 (2009) 1972-1974.
26. Y.S. Sato, H. Kokawa, Distribution of tensile property and microstructure in friction stir weld of 6063 alumium, Metall. Mater. Trans. A 32 (2001) 3023-3031.

27. K.J. Al-Fadhalah, A.I. Almazrouee, A.S. Aloraier, Microstructure and mechanical properties of multi-pass friction stir processed aluminum alloy 6063, Mater. Des. 53 (2014) 550-560.

28. E.A. El-Danaf, M.M. El-Rayes, Microstructure and mechanical properties of friction stir welded 6082 AA in as welded and post weld heat treated conditions, Mater. Des. 46 (2013) 561-572.

29. P.L. Sun, E.K. Cerreta, G.T. Gray III, and J.F. Bingert, The effect of grain size, strain rate, and temperature on the mechanical behavior of commercial purity aluminum, METAL. MATER. TRANS 37A (2006) 2983-2994.

30. M. Abdulstaar, M. Mhaede, M. Wollmann, L. Wagner, Effects of shot peening and ball-burnishing on the fatigue performance of Al 6082, 12th Int. Conf. on Shot Peening, Goslar, Germany, 2014, pp. 142-146.

31. K. Iida, Dent and affected layer produced by shot peening, 2nd Int. Conf. on Shot Peening, 1984, pp. 283-292.

32. D. Kirk, Review of shot peened surface properties, The Shot Peener, 2007, pp. 25-30.

33. K. Iida, K. Tosha, Work-softening occurred for sample processed by shot peening and grit blasting that was initially subjected to compressive strains, 1996, Conf Proc: ICSP-6, pp.296-301.

34. K. Tosha, Influence of Residual Stresses on the Hardness Number in the Affected Layer Produced by Shot Peening, 2nd Asia-Pacific Forum on Precision Surface Finishing and Deburring Technology, Seoul, Korea, 2002, pp.48-54.

List of Tables

Table 1: Tensile properties of base metal and friction stir welded material.

Condition	σ_y (0.2%), MPa	σ_{TS}, MPa	El, %
Base metal	295	323	39.2
FSW	-	166	8.1

Table 2: Average grain size and HABs in the Stir Zone of Al 6061 samples

Samples	Average grain size (standard deviation), μm			HABs, %		
	Top	Middle	Bottom	Top	Middle	Bottom
FSW	4.98 (3.17)	3.16 (2.19)	1.63 (0.70)	59.8	69.1	85.1
FSW + SP (0.18mmA)	5.10 (3.23)	3.39 (2.13)	1.80 (0.89)	64.7	69.8	81.6
FSW + SP (0.24mmA)	4.95 (3.17)	3.87 (3.01)	2.13 (1.14)	65.9	62.5	81.1

List of Figures

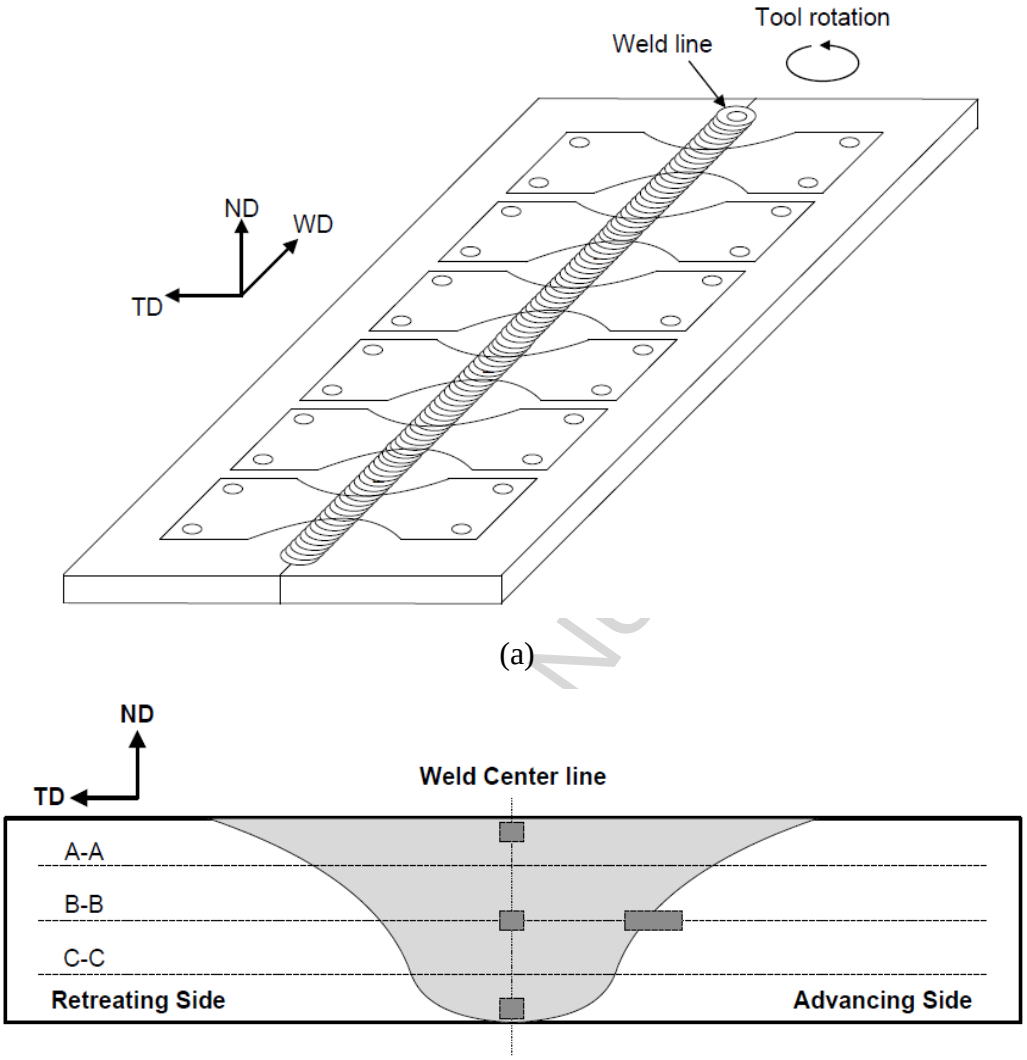

Fig. 1 Schematic illustration of FSW of AA 6061 plates: (a) Geometry of the welded plates and the fatigue specimens. The dimensions of the joint are 120 mm×300 mm and 4 mm thick.; (b) Cross-section of welded plate showing lines of measurements for microhardness (line A-A, line B-B and line C-C) and regions of EBSD measurements "dark grey boxes".

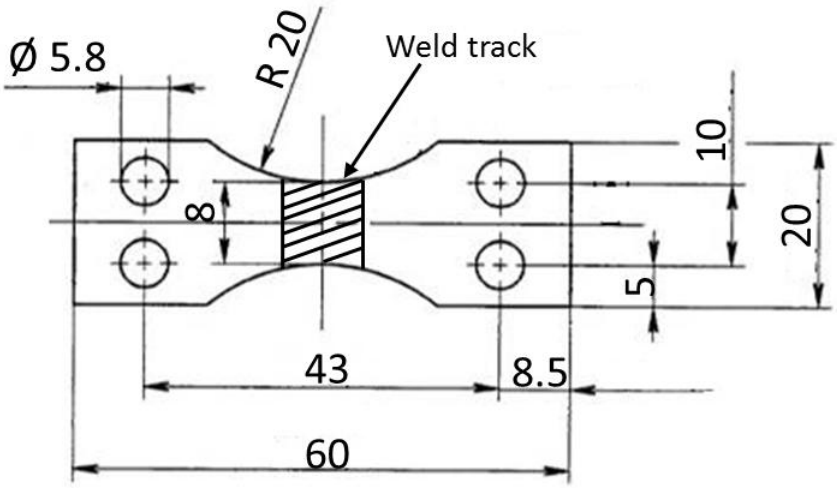

Fig. 2 Geometry of fatigue specimen, dimensions in mm.

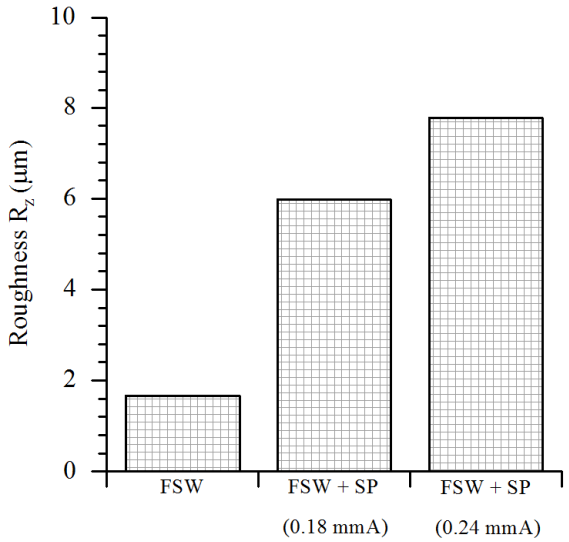

Fig. 3 Maximum roughness height (R_z) measured at different surface treatments for machined crown and root sides of 6061-T6 friction stir weld joints.

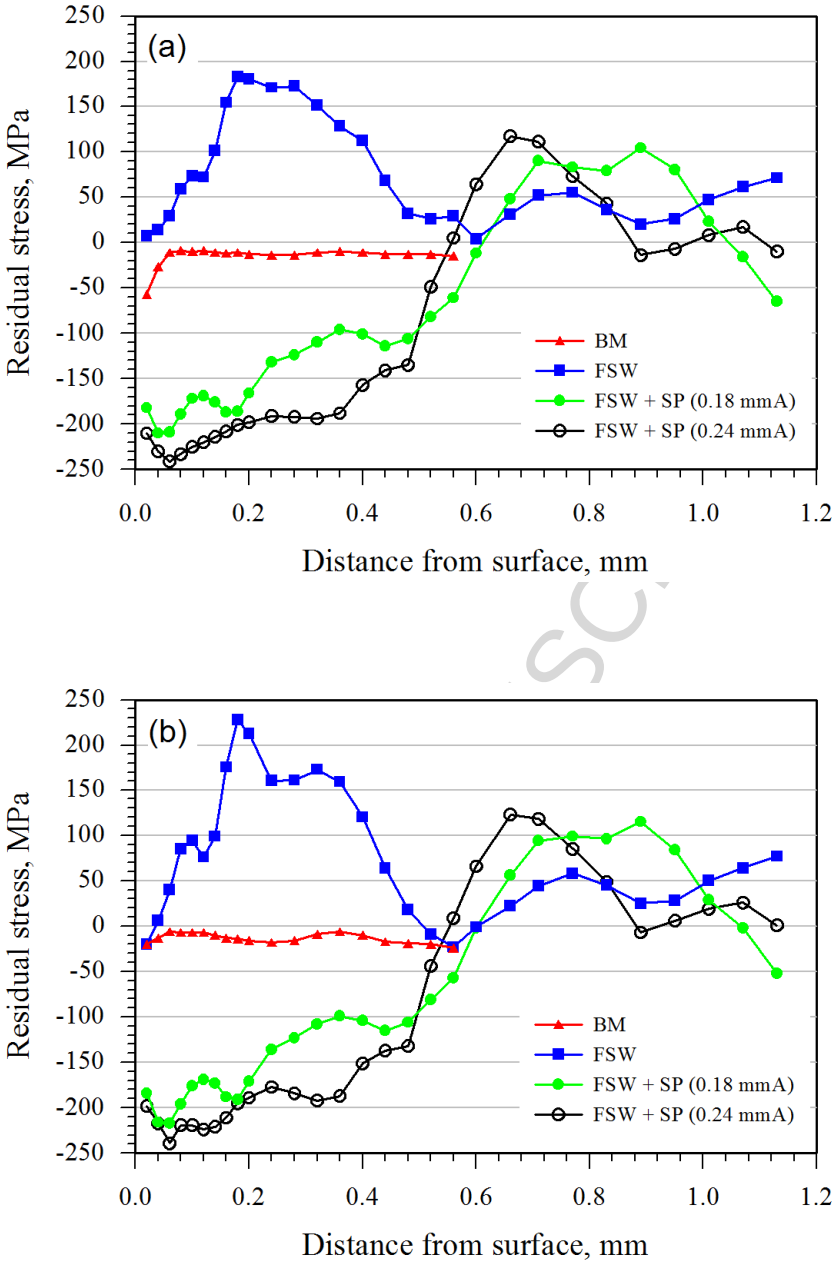

Fig. 4 Residual stress-depth profile in (a) transverse direction and (b) longitudinal direction. The residual stresses were evaluated on the crown side of the weld and at the weld centerline.

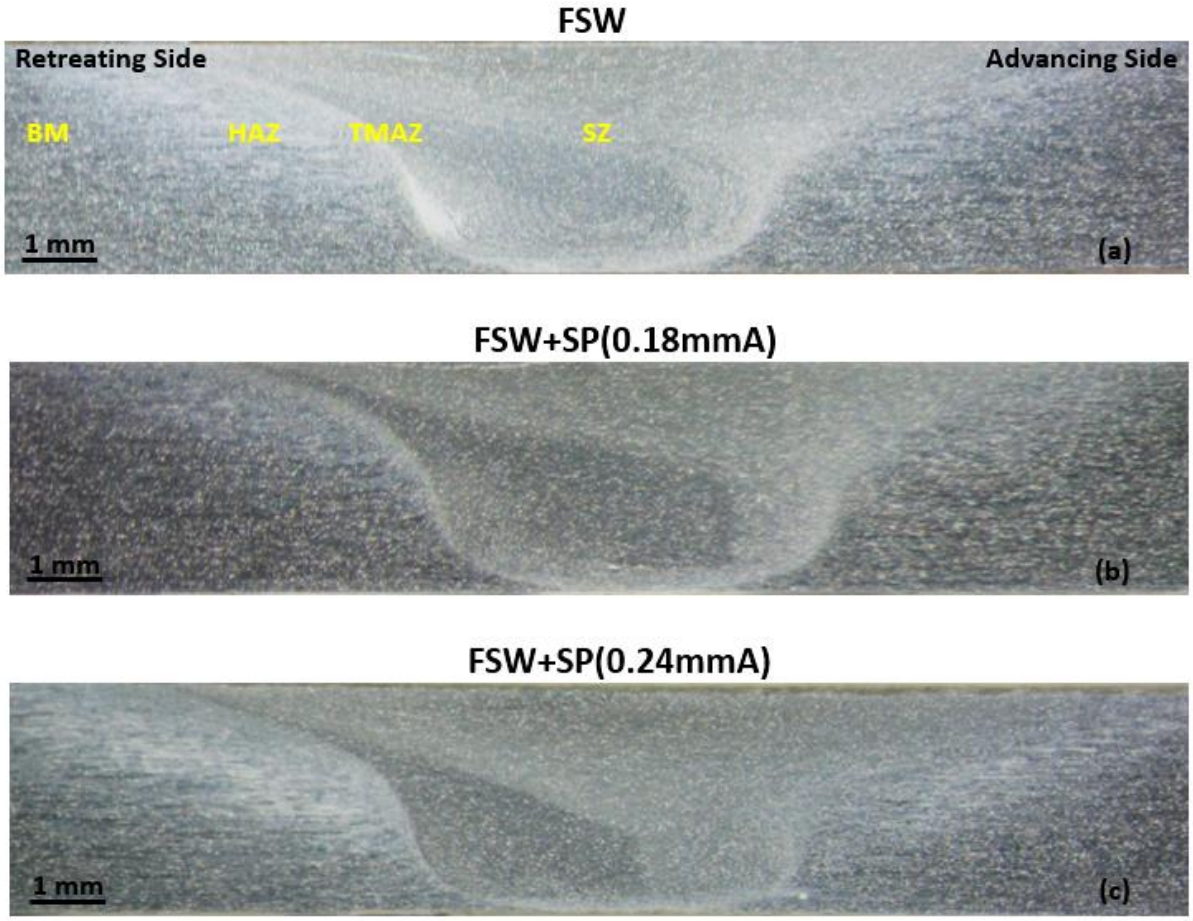

Fig. 5 Low-magnification overview of transversal cross-section of 6061-T6 weld joints: (a) FSW condition, FSW plus SP with an intensity of (b) 0.18 mmA and (c) 0.24 mmA.

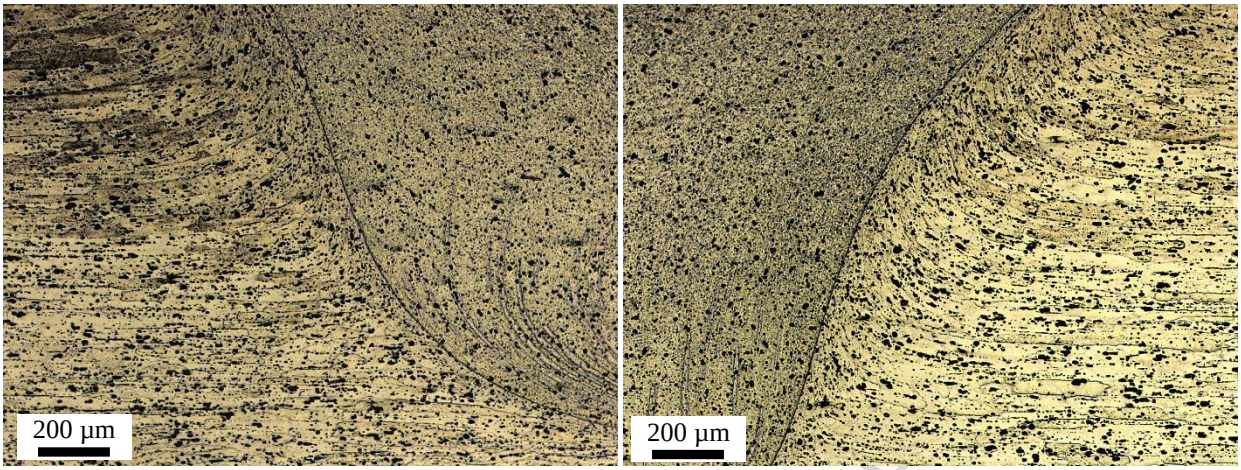

(a) (b)

Fig. 6 Optical micrographs of FSWed weld joint at the SZ-TMAZ interface: (a) Retreating side and (b) advancing side.

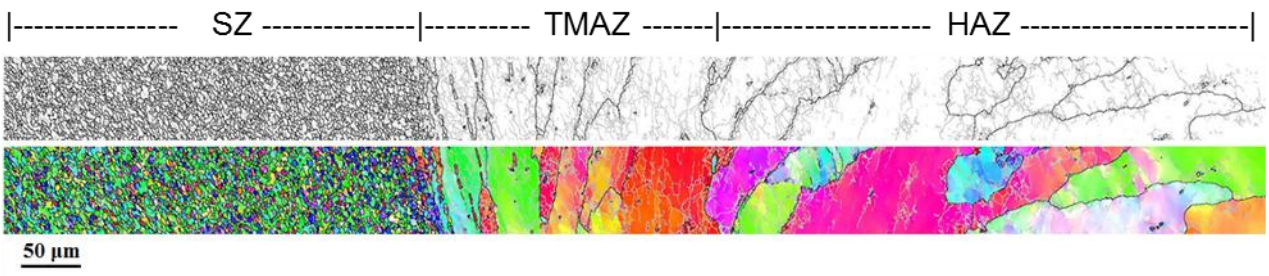

Fig. 7 Montage of EBSD maps across the SZ-TMAZ interface of the advancing side for Al 6061 samples processed by FSW.

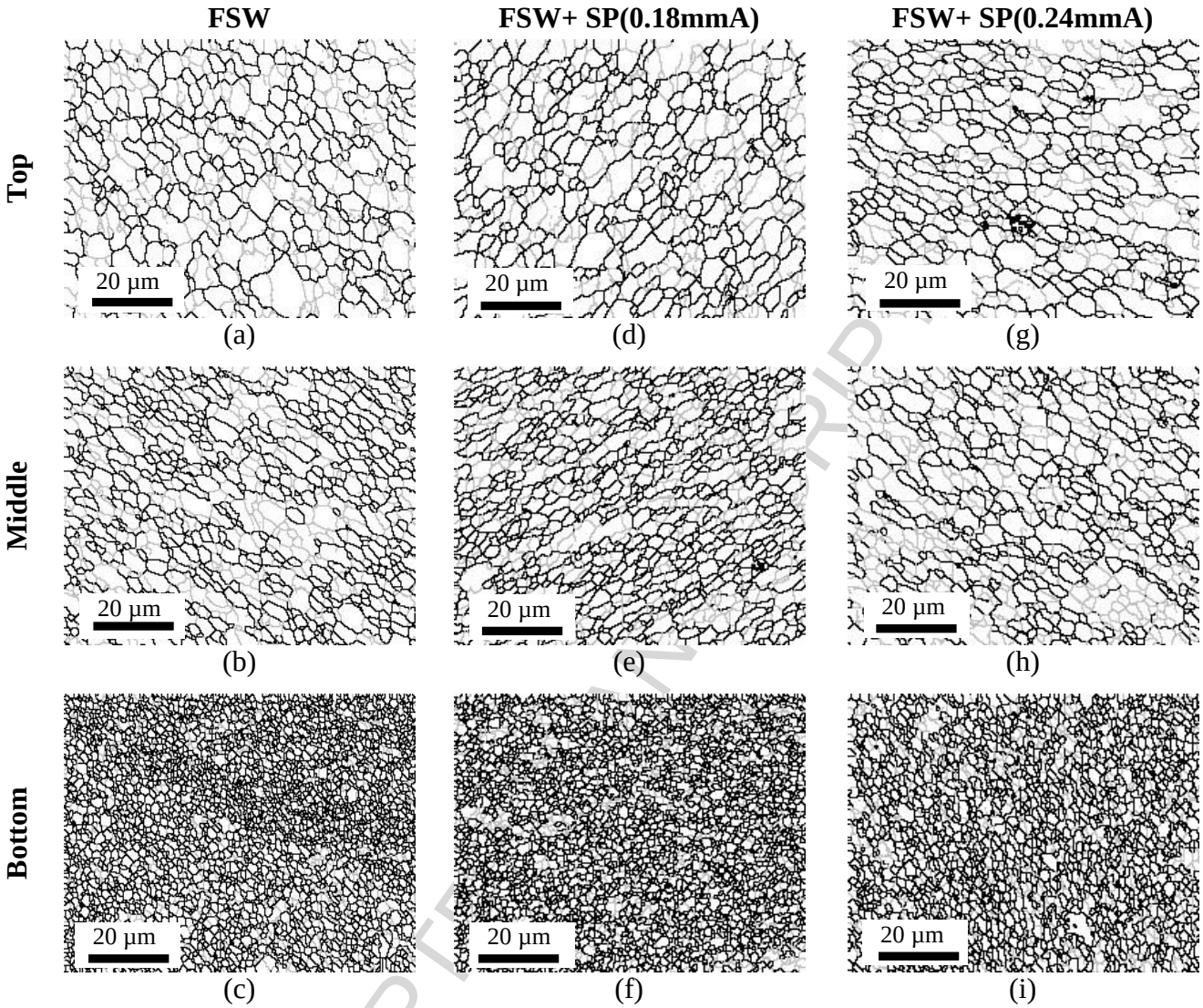

Fig. 8 Selected EBSD maps at the center line of weld for Al 6061 samples processed by: (a-c) FSW, (d-f) FSW plus shot peened with intensity of 0.18 mmA and (g-i) FSW plus shot peened with intensity of 0.24 mmA. EBSD maps were made at the top, middle and bottom regions along the center line of the weld.

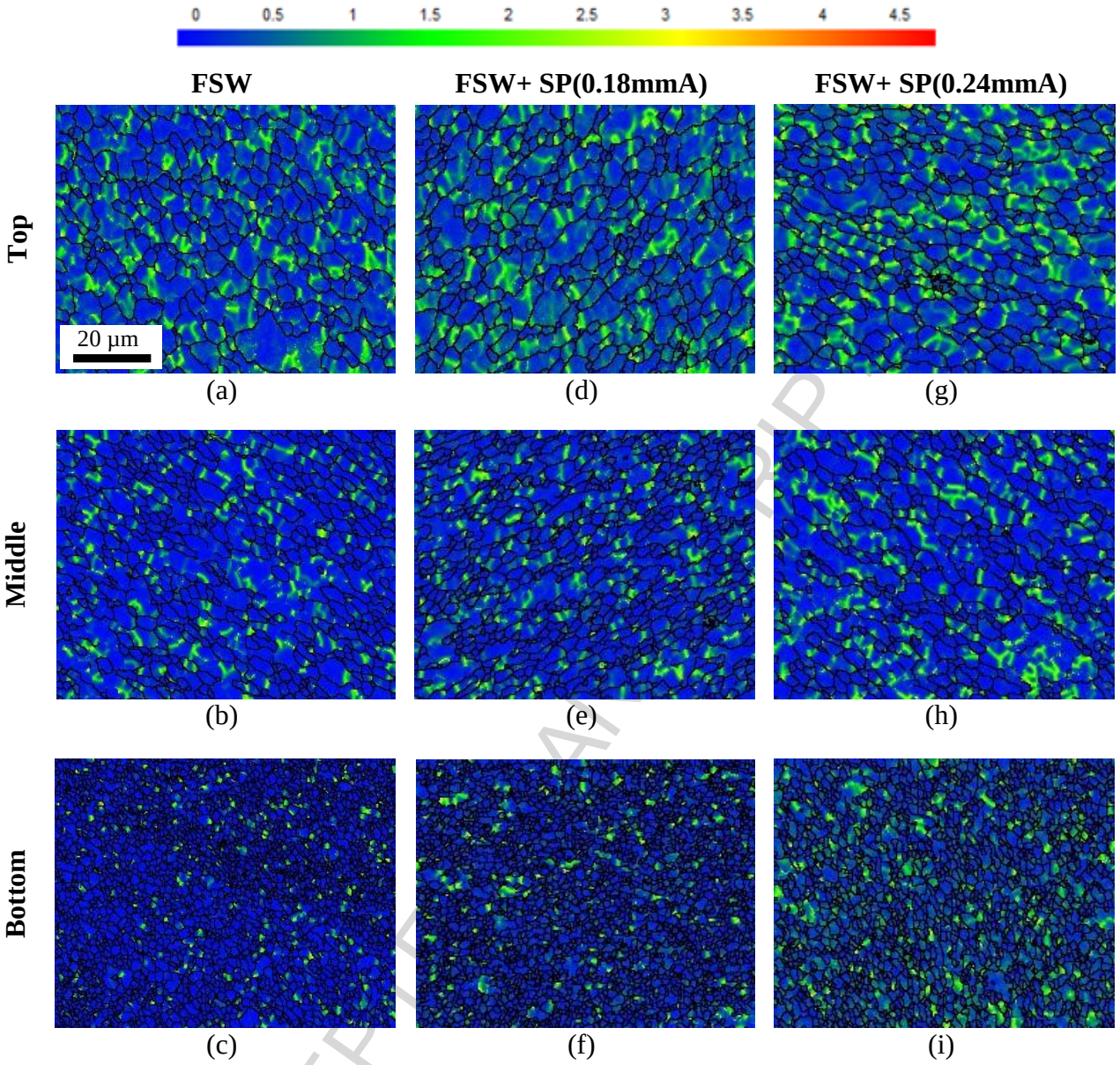

Fig. 9 Kernel average misorientation (KAM) maps at the center line of weld for Al 6061 samples processed by: (a-c) FSW, (d-f) FSW plus shot peened with intensity of 0.18 mmA and (g-i) FSW plus shot peened with intensity of 0.24 mmA.

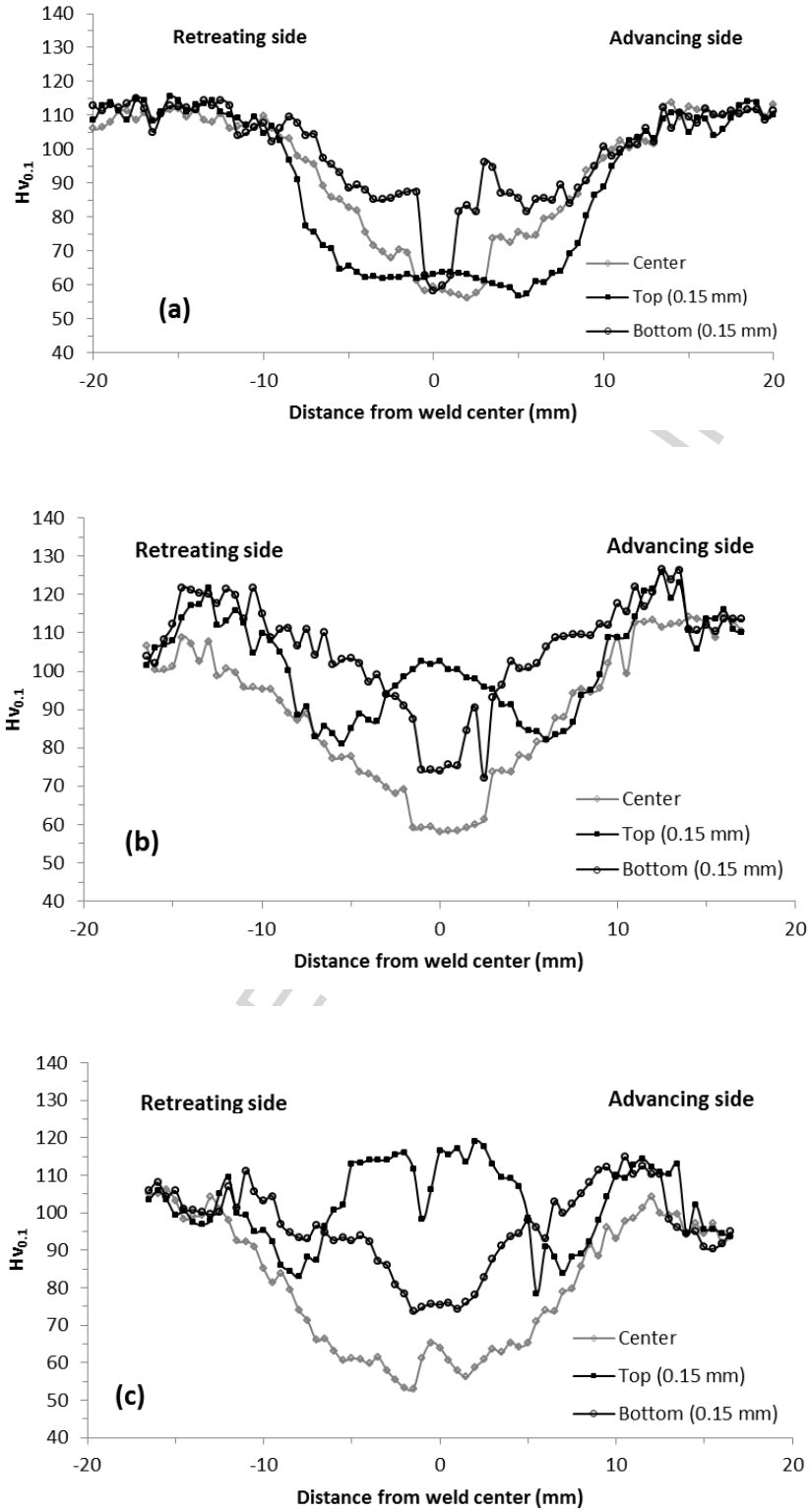

Fig. 10 Microhardness profile of the different investigated conditions: (a) FSW, (b) FSW + SP (0.18 mmA) and (c) FSW + SP (0.24 mmA).

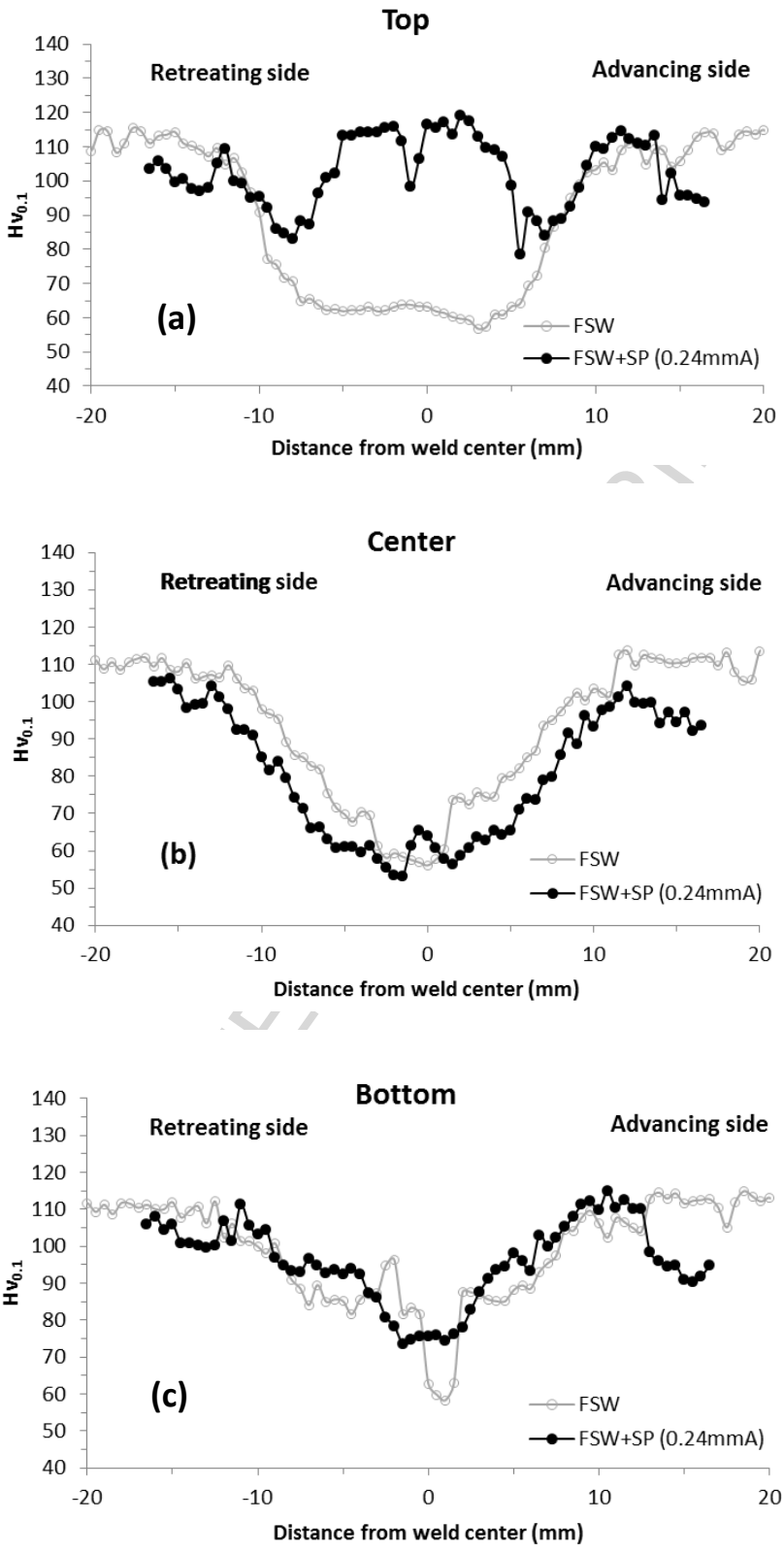

Fig. 11 Comparison of microhardness profiles of FSW and FSW+ SP (0.24 mmA).

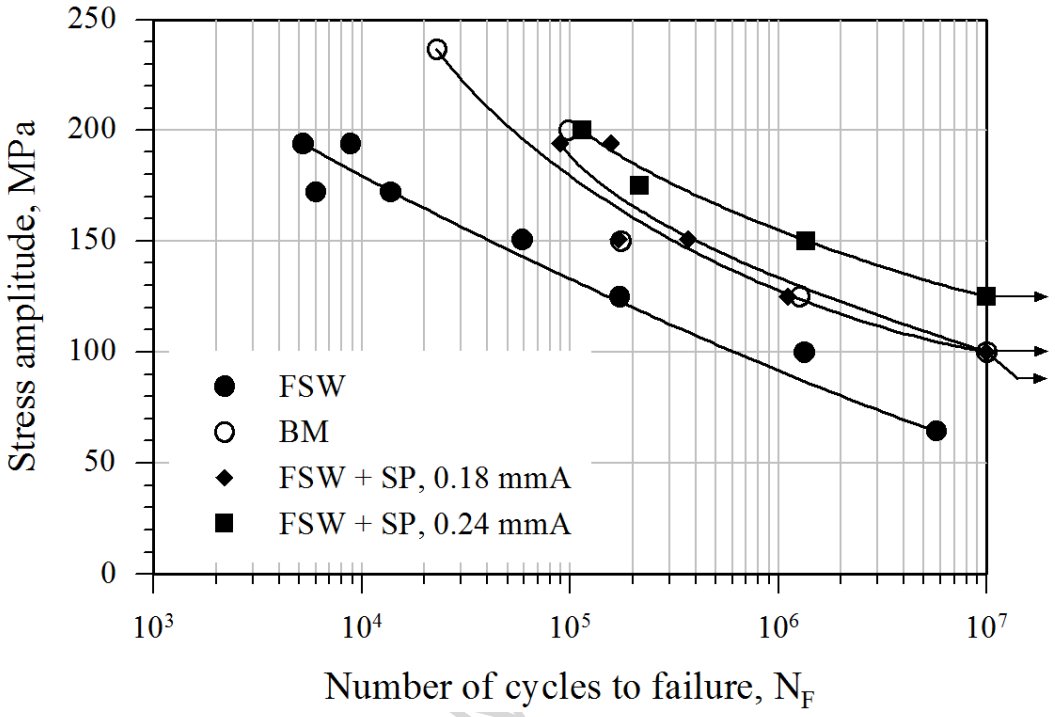

Fig. 12 Fatigue performance of various investigated conditions.

Highlights

- Grain refinement was observed after friction stir welding of AA 6061-T6.
- Reduction in microhardness and fatigue strength were obtained after welding.
- Variation in grain refinement led to different hardening behavior after peening.
- Shot peening induced beneficial compressive residual stresses.
- Shot peening and surface skimming markedly improved the fatigue performance.